Structural and spectroscopic investigations of Er^{3+} and Nd^{3+} -doped phosphate glasses

Shalini.T.K[1],Sushma.M[2*]and Hemanth Chandra.N[3]

[1]Department of Physics, Bengaluru North University,Tamaka,Kolar [2]Department of Physics, Bengaluru City University, Bengaluru [3]Department of ISC, Global Academy of Technology, Bengaluru

**Corresponding author email: sushmaphysics24@gmail.com,*

Contact No: +91 8971120094

Abstract

Phosphate glasses doped with erbium (Er^{3+}) and neodymium (Nd^{3+}) were synthesized via the melt-quenching technique to investigate their structural and optical properties for photonic applications. X- ray diffraction confirmed their amorphous nature, with a reduction in halo intensity upon doping, indicating increased structural disorder. FTIR and Raman analyses revealed that both dopants act as network modifiers, depolymerizing the phosphate network by converting Q^2 units into Q^1/Q^0 units and increasing the proportion of non-bridging oxygens. Optical absorption spectra exhibited sharp intra-4f transitions, with Er^{3+}-doped samples showing strong absorption at 547 nm and Nd^{3+}-doped samples displaying peaks at 583, 803, and 875 nm. The optical band gap decreased upon doping, reaching ~3.39 eV for Er^{3+}, suggesting enhanced defect formation. Transmittance measurements further confirmed dopant-induced optical activity, with Nd^{3+}-doped samples exhibiting broader absorption due to the richer 4f transition scheme of Nd^{3+} ions. These findings demonstrate that Er^{3+}/Nd^{3+} co-doping effectively tailors the structural and optical characteristics of phosphate glasses, enhancing their potential for solid- state laser and optical amplifier applications.

Key words: *Intra-4f electronic transitions; Non-bridging oxygen formation; $Q^2 \rightarrow Q^1/Q^0$ structural conversion*

1. Introduction

Phosphate glasses have emerged as promising materials in the field of photonics and optoelectronics owing to their distinctive physicochemical properties. These include low melting temperatures, high

thermal expansion coefficients, excellent rare-earth ion solubility, and broad optical transmission in the visible and infrared regions. The open network structure of phosphate glass matrices allows for easy incorporation of various dopants without significantly disturbing the glass-forming network. These advantages make phosphate glasses ideal for applications such as optical amplifiers, waveguides, solid- state lasers, and biomedical sensors [1,2].

Rare-earth ions such as erbium (Er^{3+}) and neodymium (Nd^{3+}) have attracted significant attention in photonic materials because of their sharp and well-defined 4f–4f electronic transitions, enabling efficient absorption and emission in the near-infrared (NIR) spectral region. Nd^{3+} ions are known for intense absorption near 803 nm and emission around 1060 nm[3], a wavelength that is vital for high-power lasers and optical communication technologies. Er^{3+} ions exhibit strong absorption around 980 nm and prominent emission at approximately 1540 nm[4], which is widely used in optical fiber amplifiers for telecommunication systems. Phosphate glasses are considered an excellent host for such ions due to their high rare-earth solubility, low phonon energy, and broad transmission range in the visible to infrared spectrum.

Although several studies have reported the optical behavior of singly doped phosphate glasses, the relationship between rare-earth ion incorporation and structural modifications of the phosphate network remains less documented. Many previous works have focused primarily on luminescent properties, giving limited attention to changes in network connectivity, such as the formation of non-bridging oxygens or the conversion between Q^2, Q^1, and Q^0 structural units [5]. Investigating these structural changes through spectroscopic techniques like Fourier-transform infrared (FTIR) and Raman spectroscopy, alongside optical absorption studies, can provide deeper insight into how Er^{3+} and Nd^{3+} ions individually influence both the local bonding environment and the overall optical response of phosphate glasses.

2. Materials and Methods:

2.1 Materials

The materials used for the synthesis of phosphate glasses included high-purity analytical-grade chemicals procured from Thermo Fisher Scientific India Pvt. Ltd. Ammonium dihydrogen phosphate ($NH_4H_2PO_4$) was used as the source of phosphorus pentoxide (P_2O_5), sodium carbonate (Na_2CO_3) served as the source of sodium oxide (Na_2O), zinc oxide (ZnO) provided ZnO content, and aluminum oxide

(Al_2O_3) was used for Al_2O_3 incorporation. For doping purposes, erbium oxide (Er_2O_3) and neodymium oxide (Nd_2O_3) were added to introduce Er^{3+} and Nd^{3+} ions, respectively, into the glass matrix. All chemicals were used as received, without further purification.

2.2 Experimental Details

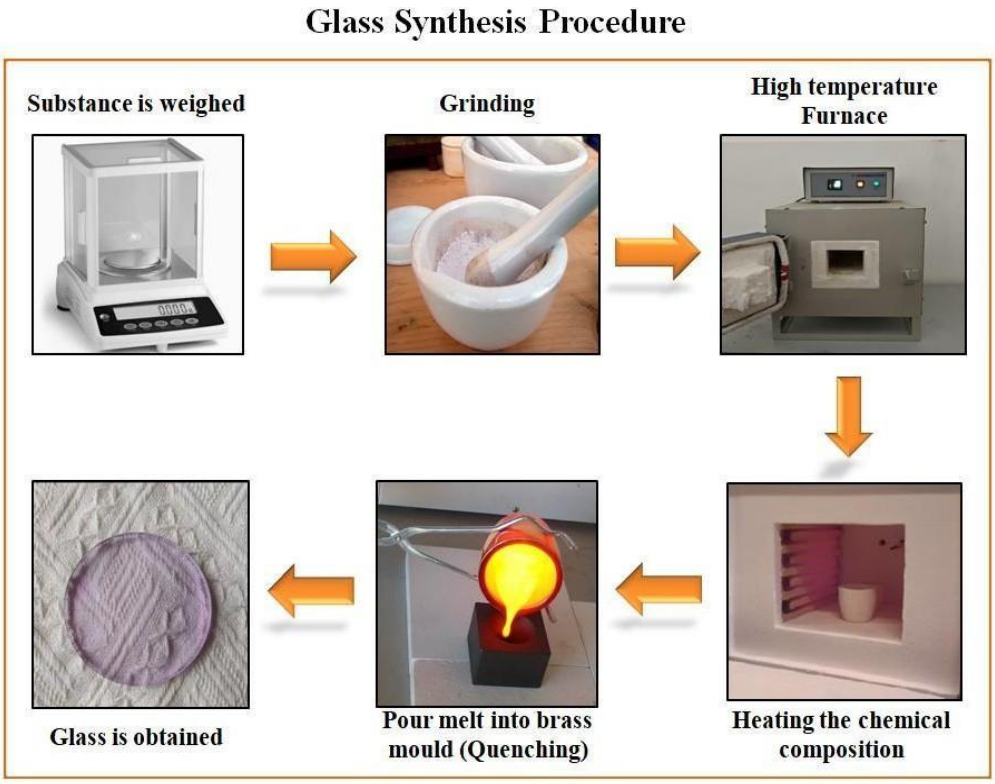

Figure 1. Step-by-step schematic of phosphate glass synthesis via the melt-quenching method

Phosphate glasses of various compositions, including undoped and rare-earth-doped samples, were synthesized using the conventional melt-quenching technique. Analytical-grade reagents with a purity of ≥99% were used as starting materials. The compositions studied included undoped ($50P_2O_5$–$5Al_2O_3$–$25Na_2O$–$20ZnO$) and the rare- earth-doped variants Er ($50P_2O_5$–$5Al_2O_3$–$20Na_2O$–$20ZnO$–$5Er_2O_3$) and Nd ($50P_2O_5$–$5Al_2O_3$–$20Na_2O$–$20ZnO$– $5Nd_2O_3$). For each batch, the required quantities (typically 14–15 g) of $NH_4H_2PO_4$, Na_2CO_3, Al_2O_3, ZnO, and either Er_2O_3 or Nd_2O_3 were accurately weighed according to the molar composition. The precursors were thoroughly ground using an agate mortar and pestle for 20–30 minutes to ensure homogeneity. The homogenized powder was then transferred to a porcelain crucible and placed in an electric muffle furnace. The temperature was raised to 1200 °C and maintained for 2 hours to ensure complete melting and homogenization of the mixture.

After melting, the viscous glass melt was poured onto a preheated metal plate (around 200 °C) to avoid thermal shock and was immediately pressed with another metal slab to form flat glass samples approximately 1–2 mm thick. The freshly formed glasses were then transferred to a preheated annealing furnace set at 350–400 °C and held for 1–2 hours to relieve internal stresses. The samples were then cooled slowly to room temperature inside the furnace at a rate of 1–2 °C/min. The final glass samples were transparent, with color variations depending on the dopant: undoped appeared colorless, while Er exhibited a pale pink hue and Nd appeared pale purple. The synthesized glasses were subsequently prepared for structural and optical characterization[6].

Table 1. Chemical compositions of phosphate glass samples doped with Er^{3+} or Nd^{3+} (mol%)

Composition of Glass	P_2O_5 %	Al_2O_3 %	Na_2O %	ZnO %	Rare earth %
undoped	50	5	25	20	0
Er	50	5	20	20	5 (Er_2O_3)
Nd	50	5	20	20	5 (Nd_2O_3)

Figure 2. Visual appearance of synthesized phosphate glass samples: undoped, Er^{3+}-doped, and Nd^{3+}-doped variants.

2.3 Instrumentation:

As-synthesized phosphate glasses doped with Er^{3+} and Nd^{3+} were characterized for their structural and optical properties. Structural analysis was carried out using X-ray diffraction (XRD) with a Malvern

PANalytical X'Pert PRO MPD system. FTIR spectra were recorded in transmittance mode for solid samples using a PerkinElmer Spectra 3 Fourier Transform Infrared Spectrometer over the range 4000– 400 cm^{-1}, while Raman spectra were obtained using a Horiba Scientific LabRAM HR Evolution Raman Spectrometer. Optical absorbance and transmittance spectra were measured using a UV-Visible-NIR spectrometer (USB4000-XR, Ocean Optics) in the wavelength range 200–1000 nm with a step size of
0.25 nm.

3. Results and Discussions:

3.1 XRD Analysis

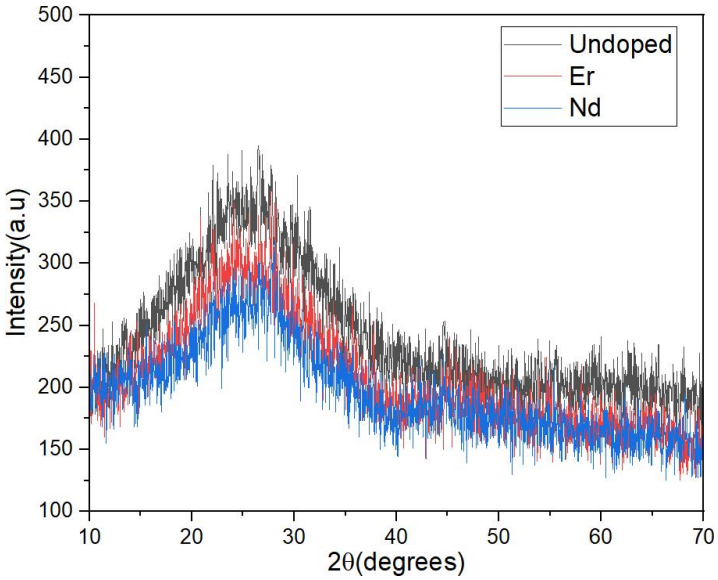

Figure 3. XRD patterns of undoped, Er^{3+}-doped, and Nd^{3+}-doped phosphate glasses confirming amorphous nature.

The XRD pattern presented shows the diffraction profiles of undoped, Er-doped, and Nd-doped phosphate glasses. All samples exhibit a broad hump centered around 2θ ≈ 25°, with no sharp crystalline peaks, indicating the amorphous nature of the glasses. This broad halo is characteristic of phosphate glasses and arises from the short-range order among atomic arrangements, such as P–O, Zn–O, and Al– O bonds, within the disordered glass network [7]. The undoped glass shows the highest intensity in the amorphous halo region, suggesting a relatively more homogeneous and compact glass structure. Upon doping with rare-earth ions like Er^{3+} and Nd^{3+}, a gradual decrease in peak intensity is observed. This reduction in intensity reflects a disruption in the glass network, likely due to the incorporation of larger trivalent rare-earth ions, which disturb the local structural arrangement. Nd-doped glass exhibits the

lowest intensity among the three, which can be attributed to the larger ionic radius of Nd^{3+} compared to Er^{3+}, leading to a greater degree of disorder[8]. Despite these changes in intensity, the position of the broad peak remains unchanged, indicating that the basic glass matrix maintains similar short-range structural features. Overall, the XRD analysis confirms that all samples remain amorphous, and rare- earth doping modifies the degree of local order without inducing crystallinity.

3.2 Infrared absorption spectra measurements Fourier-transform

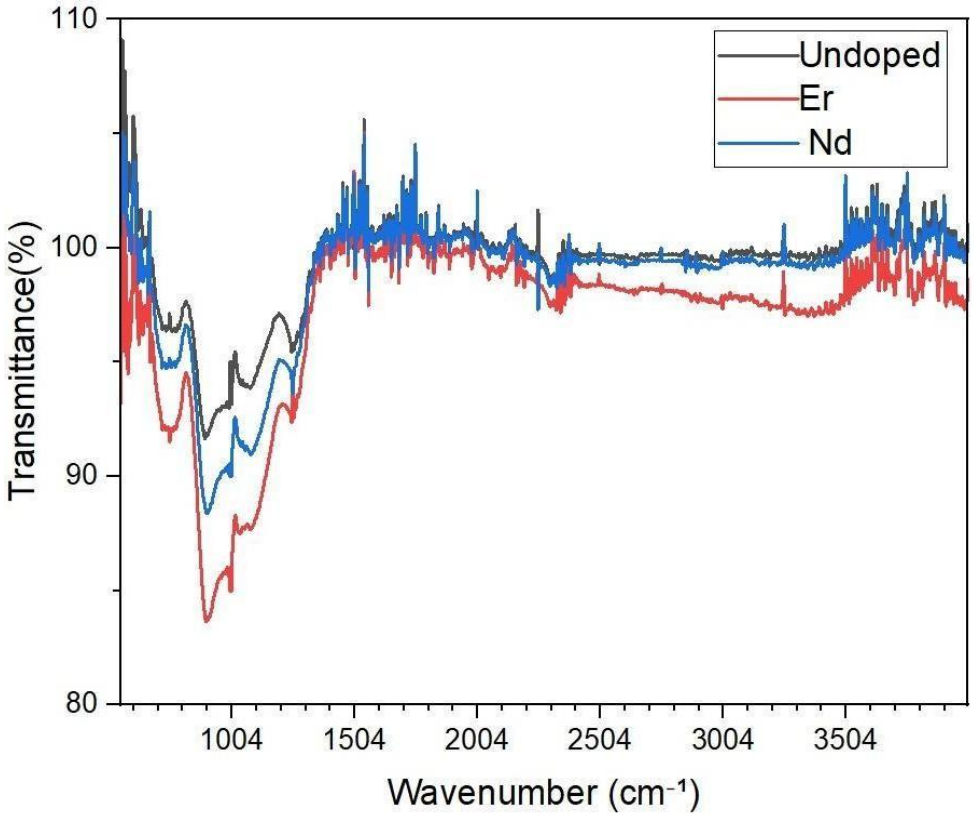

Figure 4. FTIR spectra of undoped, Er^{3+}-doped, and Nd^{3+}-doped phosphate glasses showing structural modifications in the glass network.

The FTIR spectra of the undoped and rare-earth-doped phosphate glasses in the range of 500–4000 cm^{-1} show characteristic phosphate vibrations along with the effects of doping on the glass network structure. In the undoped glass, prominent bands appear at ~1250–1150 cm^{-1} and ~900–1000 cm^{-1}, attributed respectively to asymmetric stretching of PO_2^- groups in Q^2 phosphate units and symmetric P–O–P linkages, consistent with the metaphosphate-type network. These assignments align with those reported

in literature by Brow et al. (J. Non-Cryst. Solids, 1993)[9], who established the role of PO_4 units in vibrational spectra of phosphate glasses.

Upon doping with Er^{3+} and Nd^{3+} ions, the spectra exhibit noticeable changes. There is a broadening and shift of the PO_2^- and P–O–P bands to lower wavenumbers, accompanied by a decrease in transmittance, particularly in the 1000–1200 cm^{-1} range. These effects have also been reported by El-Mallawany (Tellurite and Phosphate Glasses Handbook, 2002)[10], who noted that rare-earth ions disrupt the phosphate chains, leading to the formation of more non-bridging oxygens (NBOs**)** and transformation of Q^2 units into Q^1 or Q^0 units. The network depolymerization is thus clearly evidenced by the spectral features.

In addition, the increased intensity of a broad band around 3200–3500 cm^{-1} in the doped samples, especially for Er^{3+}, points to a higher content of structural OH^- groups or absorbed water. where rare-earth doping enhanced OH^- absorption due to increased disorder and open sites in the glass matrix. The bending vibration of H–O–H observed near ~1640 cm^{-1} supports the presence of water.Overall, it confirms that Er^{3+} and Nd^{3+} ions act as network modifiers, weakening the phosphate framework, increasing the number of NBOs, and altering the vibrational environment. The Er-doped glass shows stronger absorption and band broadening than the Nd-doped one, indicating Er^{3+} has a higher field strength and exerts a more significant influence on glass structure[7].

3.3 Raman spectroscopy

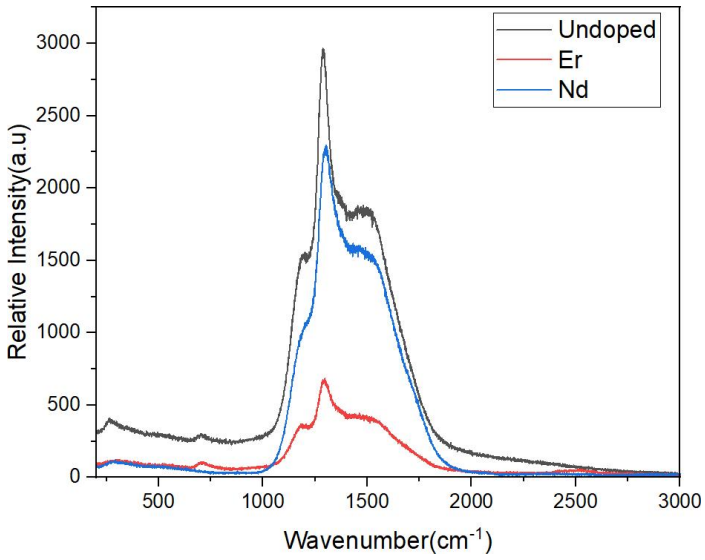

Figure 5. Raman spectra of undoped, Er^{3+}-doped, and Nd^{3+}-doped phosphate glasses highlighting changes in vibrational modes of the glass network.

The Raman spectra of undoped, Er-doped, and Nd-doped phosphate glasses exhibit broad and prominent features primarily in the 200–1800 cm^{-1} range, with a strong, intense band centered around 1300–1500 cm^{-1}, characteristic of the phosphate glass network[11]. This dominant band is attributed to the asymmetric stretching vibrations of PO_2^- groups in Q^2 units, with the highest intensity observed in the undoped glass, followed by Nd-doped and least in Er-doped samples, indicating a reduction in network polymerization due to rare-earth doping. The region from 1100–1250 cm^{-1} corresponds to symmetric stretching of PO_3^{2-} groups (Q^1 units)[12], and its slight enhancement in doped glasses—particularly in the Nd-doped sample—suggests network depolymerization. The 700–900 cm^{-1} range, related to P–O–P symmetric stretching, reveals subtle features reflecting changes in bridging oxygen linkages caused by dopant incorporation[13]. Bands within 400–600 cm^{-1} are associated with O–P–O bending and potential Zn–O or Al–O interactions, indicating dopant-related structural modifications. Finally, modes below 400 cm^{-1} are attributed to lattice vibrations and metal–oxygen bonds, such as Er–O and Nd–O, which manifest as weak features or small shoulders, further confirming the structural influence of rare-earth elements on the phosphate glass matrix.

3.4 UV–visible absorption measurements

The absorption spectra of undoped and rare-earth-doped phosphate glass samples in the wavelength range of 200–1100 nm are shown in the figure. All samples exhibit strong absorption below approximately 300 nm, which is characteristic of the ultraviolet (UV) absorption edge of the phosphate glass matrix [14]. This behavior arises due to electronic transitions involving P–O, Zn–O, and Al–O bonds. Beyond ~350 nm, the undoped glass shows a largely featureless spectrum, with nearly flat absorbance in the visible and near-infrared (NIR) regions. In contrast, sharp absorption peaks appear in the Er^{3+}- and Nd^{3+}-doped glasses, confirming the successful incorporation of rare-earth ions into the glass matrix.

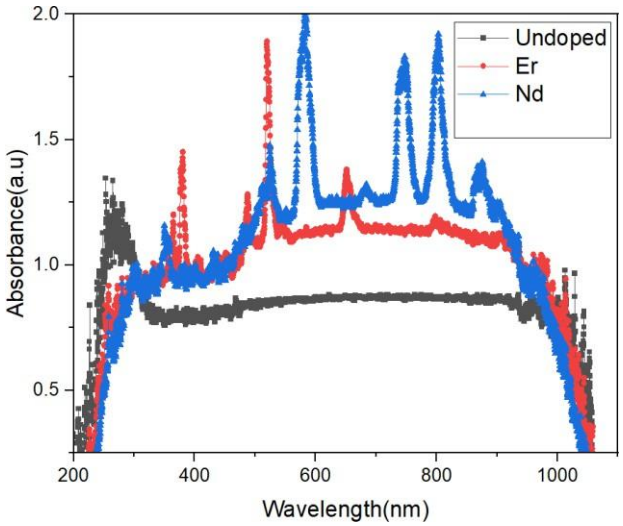

Figure 6. UV–Visible absorbance spectra of undoped, Er^{3+}-doped, and Nd^{3+}-doped phosphate glasses showing characteristic absorption bands.

When **Erbium ions (Er^{3+})** are doped into the glass composition $25Na_2O + 50P_2O_5 + 20ZnO + 5Al_2O_3$, they occupy interstitial or modifier sites within the glass network [15]. Phosphate glass is particularly suitable for rare-earth doping due to its **low phonon energy**, which reduces non- radiative decay, **high solubility for rare-earth ions without clustering**, and **optical transparency in the UV–NIR range**, which allows clear detection of Er^{3+} transitions. Several sharp absorption peaks are observed, superimposed on the broad background from the host matrix. These peaks correspond to intra-4f transitions of Er^{3+} from the ground state $^4I_{15/2}$ to various excited states. These features are absent in the undoped sample, confirming that the absorption bands originate from the Er^{3+} ions and not from the host glass. Among these, the peak around **547 nm** ($^4I_{15/2} \rightarrow {}^4S_{3/2}$) is the most prominent and is commonly used to verify the presence of Er^{3+} ions. While absorbance increases toward the UV region due to the host glass, the Er^{3+}-related peaks are sharper and occur at specific wavelengths due to 4f–4f electronic transitions.

Table 2. Characteristic absorption peaks of Er^{3+}-doped phosphate glasses with corresponding electronic transitions, spectral regions, and typical applications

Wavelength (nm)	Transition	Region	Application
520 nm	$^4I_{15/2} \rightarrow {}^2H_{11/2}$	Green	Medium intensity
547 nm	$^4I_{15/2} \rightarrow {}^4S_{3/2}$	Green	**Strongest Er^{3+} peak is visible**
652 nm	$^4I_{15/2} \rightarrow {}^4F_{9/2}$	Red	Commonly observed in Er^{3+} glass
800,908,972 nm	$^4I_{15/2} \rightarrow {}^4I_{11/2}, {}^4I_{13/2}$	NIR	Infrared emission regions

In the case of **Nd^{3+}-doped glass**, multiple sharp absorption peaks appear in the 400–900 nm range. These arise from intra-4f transitions of Nd^{3+} ions from the ground state $^4I_{9/2}$ to various excited levels. The most intense absorption in the visible region typically appears around **580– 590 nm**[16], followed by strong peaks in the **740–880 nm** region of the NIR spectrum. These transitions highlight the potential of Nd^{3+}-doped glasses for **near-infrared laser and optical amplifier applications**, owing to their efficient absorption characteristics in technologically important spectral regions.

Table 3. Characteristic absorption peaks of Nd^{3+}-doped phosphate glasses with corresponding electronic transitions, spectral regions, and typical applications

Approx. Wavelength (nm)	Transition	Region	Application
524 nm	$^4I_{9/2} \rightarrow {}^2G_{7/2} + {}^4G_{9/2}$	Green	Moderate intensity
583 nm	$^4I_{9/2} \rightarrow {}^4G_{5/2} + {}^2G_{7/2}$	Yellow- orange	**Strongest visible Nd^{3+} peak**
746 nm	$^4I_{9/2} \rightarrow {}^4F_{7/2} + {}^4S_{3/2}$	Red-NIR	Strong absorption in laser range
803 nm	$^4I_{9/2} \rightarrow {}^4F_{5/2} + {}^2H_{9/2}$	NIR	Pump band for 1064 nm laser emission
875 nm	$^4I_{9/2} \rightarrow {}^4F_{3/2}$	NIR	Strong pump transition for Nd lasers

3.4.1 Transmittance Spectra of Undoped and Er^{3+}/Nd^{3+}-Doped Phosphate Glasses

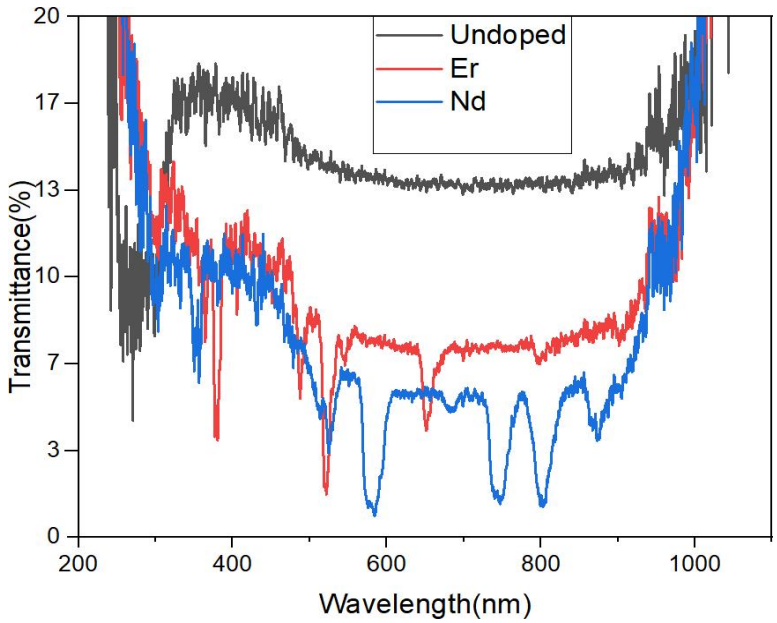

Figure 7. UV–Vis–NIR transmission spectra of undoped, Er^{3+}-doped, and Nd^{3+}-doped phosphate glasses

The transmittance spectra of undoped, Er^{3+}-doped, and Nd^{3+}-doped phosphate glass samples in the wavelength range of 200–1100 nm reveal clear differences in optical behavior. The undoped glass exhibits the highest overall transmittance, remaining largely featureless beyond 350 nm, with a strong absorption edge below 300 nm due to intrinsic electronic transitions within the phosphate glass network (such as P–O, Zn–O, and Al–O bonds). In contrast, the Er^{3+}-doped
sample shows reduced transmittance across the visible and NIR regions, along with distinct sharp absorption bands at specific wavelengths—most notably near 547 nm and 980 nm—corresponding to intra-4f transitions from the ground state
$^4I_{15/2}$ of Er^{3+} to excited states. The Nd^{3+}-doped glass displays the lowest transmittance overall and exhibits multiple pronounced absorption bands in the 400–900 nm range, especially near 580–590 nm, 740 nm, and 800–880 nm, which correspond to characteristic intra-4f transitions of Nd^{3+} ions. These spectral features confirm the successful incorporation of rare-earth ions into the glass matrix, with Nd^{3+} introducing more extensive absorption than Er^{3+} due to its richer 4f transition structure. The comparison demonstrates that rare-earth doping significantly modifies the optical properties of phosphate glass, enhancing its

potential for photonic and laser applications in the visible and NIR regions[17].

3.4.2 Optical Band Gap of Undoped and Er^{3+}/Nd^{3+}-Doped Phosphate Glasses

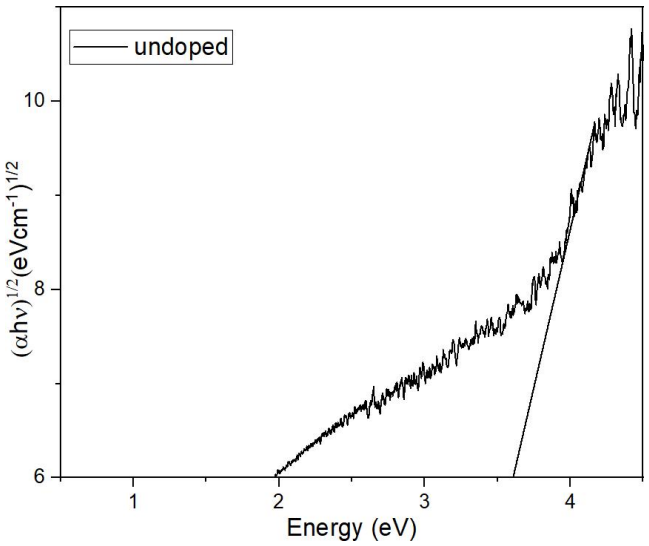

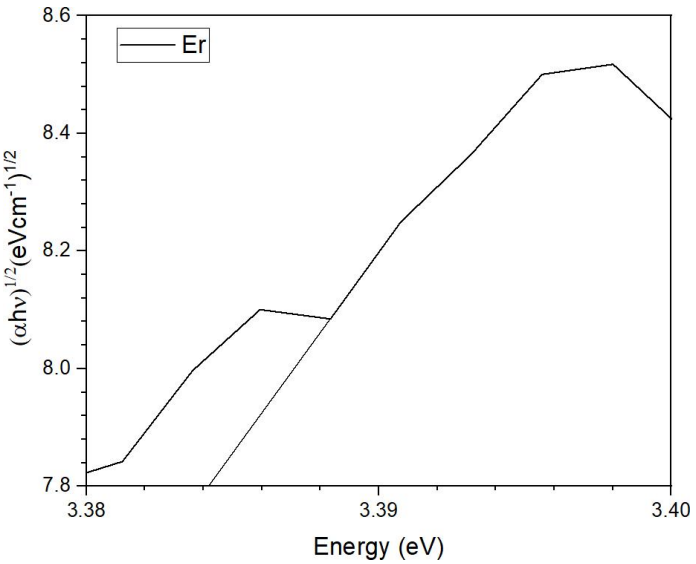

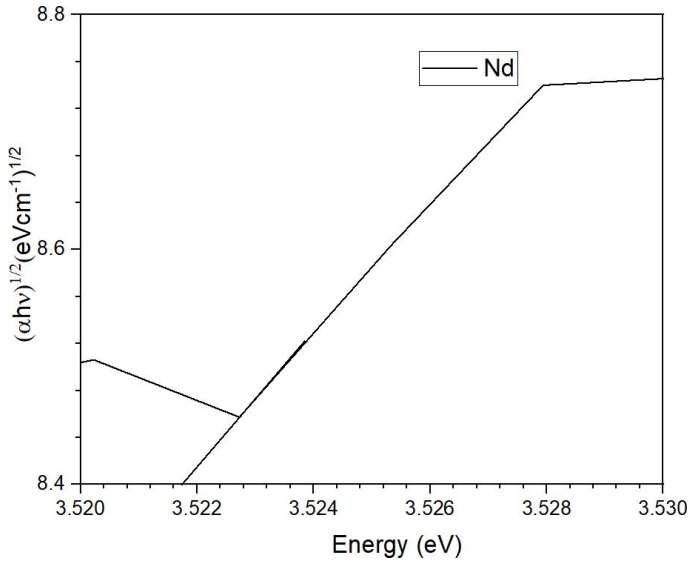

Figure 8. Tauc Plots for Optical Band Gap Determination of undoped,Er and Nd doped Phosphate Glass

The **undoped glass** exhibits the typical behavior of phosphate glasses, characterized by a relatively wide optical band gap. This is due to the absence of impurity levels or localized states within the band structure, allowing only intrinsic electronic transitions. Upon doping with **Nd^{3+} ions**, the glass matrix is modified through the introduction of intermediate 4f energy levels within the band gap. These additional states facilitate new optical absorption pathways, thereby lowering the energy required for electronic transitions. As a result, the optical indirect band gap decreases by approximately **0.6 eV** compared to the undoped glass [18, 19]. In the case of **Er^{3+} doping**, the incorporation of erbium ions causes further structural distortion in the glass network and introduces more defect energy levels. These defects promote even lower energy transitions than those introduced by Nd^{3+} ions. Consequently, the **Er^{3+}-doped glass exhibits the lowest indirect band gap**, around **3.39 eV**, which corresponds to a reduction of about **0.7 eV** compared to the undoped sample [20].

4. Conclusion

This study investigates the effect of Er^{3+} and Nd^{3+} doping on the structural and optical properties of phosphate glasses. All samples maintained their amorphous character, but spectroscopic analysis showed that these rare-earth ions act as network modifiers, causing depolymerization of the phosphate framework by breaking Q^2 units and increasing non-

bridging oxygen content. These structural changes directly influence optical behavior, producing sharp intra-4f absorption bands and a decrease in both optical band gap and transmittance. The results confirm successful incorporation of Er^{3+} and Nd^{3+} and their role in modifying the glass network. The distinct absorption features in the visible and near-infrared regions suggest potential applications in optical amplifiers, waveguides, and solid-state lasers. Notably, Er^{3+} induces stronger structural rearrangements, whereas Nd^{3+} generates broader and more intense optical absorption.

Credit authorship contribution statement

Shalini.T.K, Sushma M: Investigation, analysis, Methodology, writing- original draft, review and editing.

Hemanth Chandra.N: Conceptualization, Validation, Supervision, editing.

Declaration of competing interest:

This research did not receive any specific grant from funding agencies in the public, commercial, or not-for-profit sectors.

References:

1. Mandlule, Armando, Franziska Döhler, Leo Van Wüllen, Toshihiro Kasuga, and Delia S. Brauer. 2014. "Changes in Structure and Thermal Properties with Phosphate Content of Ternary Calcium Sodium Phosphate Glasses." *Journal of Non-Crystalline Solids* 392–393: 31–38. https://doi.org/10.1016/j.jnoncrysol.2014.04.002.
2. Ehrt, Doris. 2015. "Phosphate and Fluoride Phosphate Optical Glasses - Properties, Structure and Applications." *Physics and Chemistry of Glasses: European Journal of Glass Science and Technology Part B* 56 (6): 217–34. https://doi.org/10.13036/17533562.56.6.217.
3. Rosal, B. del, U. Rocha, E. C. Ximendes, E. Martín Rodríguez, D. Jaque, and J. García Solé. 2017. "Nd3+ Ions in Nanomedicine: Perspectives and Applications." *Optical Materials* 63: 185–96. https://doi.org/10.1016/j.optmat.2016.06.004.
4. Li, Leipeng, Yuan Zhou, Feng Qin, Yangdong Zheng, and Zhiguo Zhang. 2020. " On the Er 3+ NIR Photoluminescence at 800 Nm ." *Optics Express* 28 (3): 3995. https://doi.org/10.1364/oe.386792.
5. Almulhem, Najla Khaled, Hayat H Almulhim, M A Farag, and Aly Saeed. 2025. "In Oxyfluorophosphate Glass," 1–16.
6. El-Maaref, A. A., Shimaa Badr, Kh S. Shaaban, E. A. Abdel Wahab, and M. M. ElOkr. 2019. "Optical Properties and Radiative Rates of Nd 3+ Doped Zinc-Sodium

Phosphate Glasses." *Journal of Rare Earths* 37 (3): 253–59. https://doi.org/10.1016/j.jre.2018.06.006.

7. Sallam, O. I., Abdel Maksoud, M. I. A., Kassem, S. M., Awed, A. S., & Elalaily, N. A. (2022). Enhanced linear and nonlinear optical properties of erbium/ytterbium lead phosphate glass by gamma irradiation for optoelectronics applications. *Applied Physics A: Materials Science and Processing*, *128*(9). https://doi.org/10.1007/s00339- 022-05965-4
8. Hegde, V., Vighnesh, K. R., Kamath, S. D., Viswanath, C. S. D., Almuqrin, A. H., Sayyed, M. I., Gangareddy, J., Rajaramakrishna, R., & Keshavamurthy, K. (2024). Near-infrared and green light emission spectroscopic characteristics of Er3+ doped alumina–phosphate glasses. *Applied Physics A: Materials Science and Processing*, *130*(6). https://doi.org/10.1007/s00339-024-07531-6
9. Brow, R. K., Tallant, D. R., Hudgens, J. J., Martin, S. W., & Irwin, A. D. (1994). The short-range structure of sodium ultraphosphate glasses. In *Journal of Non-Crystalline Solids* (Vol. 177).
10. El-Mallawany, R. (2003). *Glass transformation temperature and stability of tellurite glasses*. http://journals.cambridge.org
11. Schwarz, J., H. Tichá, L. Tichý, and R. Mertens. 2004. "Physical Properties of PbO- ZnO-P2O5 Glasses I. Infrared and Raman Spectra." *Journal of Optoelectronics and Advanced Materials* 6 (3): 737–46.
12. Jiménez, José A. 2024. "Holistic Assessment of NIR-Emitting Nd3+-Activated Phosphate Glasses: A Structure-Property Relationship Study." *ACS Organic and Inorganic Au* 4 (3): 338–49. https://doi.org/10.1021/acsorginorgau.3c00071.
13. Li, Baiyi, and Guangdong Zhou. 2025. "Preparation of Phosphate Glass by the Conventional and Microwave Melt-Quenching Methods and Research on Its Performance." *Materials* 18 (5). https://doi.org/10.3390/ma18051079.
14. H.A. ElBatal.(2011). UV–visible and infrared absorption spectra of gamma irradiated CuO- doped lithium phosphate, lead phosphate and zinc phosphate glasses: A comparative study. https://www.sciencedirect.com/journal/physica-b-condensed-matter, 0921-4526, 3694–3703. doi:10.1016/j.physb.2011.06.074
15. Saddam Hussain.(2017). Optical Investigation of Sm3+ Doped in Phosphate Glass. Glass Physics and Chemistry, 1087-6596, Vol. 43, No. 6, pp. 538–547, DOI: 10.1134/S1087659617060219.

16. G. Neelima(2018). Investigation of optical and spectroscopic properties of neodymium doped oxyfluoro-titania-phosphate glasses for laser applications, ScriptaMaterialia162,246–250, https://doi.org/10.1016/j.scriptamat.2018.11.018

17. Sendova, Mariana, and José A. Jiménez. 2021. "Band Gap Analysis and Correlation with Glass Structure in Phosphate Glasses Melted with Various Allotropes of Carbon." *Chemical Physics* 547 (April). https://doi.org/10.1016/j.chemphys.2021.111207.

18. M.R. Dousti, (2020) Tungsten sodium phosphate glasses doped with trivalent rare earth ions (Eu3+,Tb3+,Nd3+ and Er3+) for visible and near-infrared applications,Journal of Non- Crystalline Solids 530, 119838, 0022-3093, https://doi.org/10.1016/j.jnoncrysol.2019.119838

19. M. S. Sadeq.(2021), The tungsten oxide within phosphate glasses to investigate the structural, optical, and shielding properties variations, J Mater Sci: Mater Electron, https://doi.org/10.1007/s10854-021-05871-0

20. H. Es-souf. (2021), Effect of TiO2 on the chemical durability and optical properties of Mo- based phosphate glasses Journal of Non-Crystalline Solids 558, 120655, 0022-3093, https://doi.org/10.1016/j.jnoncrysol.2021.120655